Mechanics and Mechanical Engineering
Vol. 22, No. 2 (2018) 553–564

https://doi.org/10.2478/mme-2018-0044

Efficiency Optimisation of Blade Shape in Steam and ORC Turbines

Piotr Lampart
Łukasz Witanowski
Piotr Klonowicz
The Szewalski Institute of Fluid Flow Machinery
Polish Academy of Sciences
Gdańsk, Poland
piotr.lampart@imp.gda.pl
lukasz.witanowski@imp.gda.pl
piotr.klonowicz@imp.gda.pl

Received (23 June 2018)
Revised (19 August 2018)
Accepted (23 August 2018)

This paper is devoted to direct constrained optimisation of blading systems of large power and small power turbines so as to increase their internal efficiency. The optimisation is carried out using hybrid stochastic-deterministic methods such as a combination of a direct search method of Hooke-Jeeves and simulated annealing or a combination of a bat algorithm and simplex method of Nelder-Mead. Among free shape parameters are blade number and stagger angle, stacking blade line parameters and blade section (profile) parameters.

One practical example of efficiency optimisation of turbine blading systems is modification of low load profiles PLK-R2 for high pressure (HP) stages of large power steam turbines. Another optimised geometry is that of an ORC radial-axial cogeneration turbine of 50 kWe. Up to 1% efficiency increase can easily be obtained from optimisation of HP blade profiles, especially by making the rotor blade more aft-loaded and reducing the intensity of endwall flows. Almost 2% efficiency rise was obtained for the optimised 50 kWe ORC turbine due to flow improvement at the suction side of the blade.

Keywords: steam turbine, ORC turbine, blading systems, optimisation, total enthalpy loss.

1. Introduction

Efficiency of power plants (heat and power plants) is crucial for the profitability of electric energy production and reduction of emissions to the environment. In Rankine cycles an increase of energy efficiency can be possible thanks to perfection of thermodynamic cycle, increasing cycle parameters and increasing internal efficiency of turbines.

Currently, supercritical steam units ($p_0 = 30$ MPa and $t_0 = 610/620$°C) reach an efficiency of 46% [1]. An increase in live or reheat steam temperature by 20^{o}C is possible and expected to raise the steam cycle efficiency by 1% point. Also an increase of turbine efficiency can be obtained eg. via optimisation of turbine flow passages, including classical optimisation of stator and rotor blade numbers and stagger angles, optimisation of labyrinth seal geometries to reduce leakage flows through technological clearances as well as optimisation of blade sections (profiles), endwalls and blade stacking lines.

Due to a large number of geometry parameters of turbine flow domains and large costs of flow computations, effective optimisation strategies are required. The objective function to be optimised assumed in this paper is the total enthalpy loss of the turbine stage obtained from a RANS solver, whose calculation is the largest cost during optimisation. Therefore, approximate models to calculate the objective function such as an artificial neural network trained over a data base of high-fidelity 3D RANS solutions are often used [2]. Direct optimisation methods, especially those using hybrid stochastic-deterministic algorithms are also effective both for single-extremum and multimodal objective functions [3]. Equally important in optimisation tasks from the field of turbine flow systems is knowledge of loss mechanisms [4], which enables proper selection of optimisation parameters.

In this paper an idea of direct constrained optimisation of turbine flow geometry is developed. Two stochastic-deterministic optimisation methods are described - a direct search method of Hooke-Jeeves combined with simulated annealing as well as a combination of a bat algorithm with simplex method of Nelder-Mead. Two methods of parametrisation of the blade profile are used – based on a set of circle arcs and Bezier functions.

In the course of optimisation described in this paper turbine blade profiles and/or endwall contours are optimised. Change of the blade profile redistributes profile load and changes the state of boundary layers at the suction surface, thus changes the distribution of profile loss and gives a chance to reduce it. The redistribution of profile load also has an effect on redistribution and reduction of endwall/secondary flow losses. More efficiency gains due to reduction of endwall/secondary flow losses can be attributed to optimisation of 3D blade stacking lines [5-7].

2. Direct constrained optimisation of turbomachinery blading systems

Optimisation is an iterative procedure that seeks for an extremum of the objective function:

$$min_x f(\mathbf{y}(\mathbf{x}), \mathbf{x}) \quad \text{or} \quad max_x f(\mathbf{y}(\mathbf{x}), \mathbf{x})$$

assuming that: $\mathbf{y} \in [\mathbf{y}_{\min}; \mathbf{y}_{\max}]$; $\mathbf{x} \in [\mathbf{x}_{\min}; \mathbf{x}_{\max}]$, where f is an objective function, $\mathbf{y}$ – vector of assumed flow parameters; $\mathbf{x}$ – vector of assumed geometrical parameters. In this work, the objective function is built based on the flow loss coefficient, defined as the total enthalpy loss of the turbine stage obtained from CFD computations with the leaving energy:

$$f = \xi$$

Optimisation of blading systems should be conducted as constrained optimisation. Constraints refer both to geometric parameters which are optimised as well

as to flow and structure parameters which are not directly optimised so as to assure that they do not fall beyond the allowed range of variation. The following sample flow/structure parameters can be considered during optimisation: exit flow angle, mean reaction, reaction at the root and tip, mass flow rate and stresses in the metal.

Geometric and flow parameters can be constrained in two ways. Stiff constraints are used with respect to the exit angle, reactions and stresses in the metal, meaning that the objective function acquires a certain large value if the allowed range of variation of these parameters is exceeded:

$f = \xi$ – if the parameters fall within the allowed range of variation,
$f = \infty$ – otherwise or if flow calculations do not converge.

Beside stiff constraints, weak constraints are also used and usually applied to the mass flow rate (resultant for a flow solver assuming the pressure drop across the stage as a boundary condition). For this constraint a penalty is assigned to the objective function if a flow characteristic falls beyond the required interval $[G_-, G_+]$ around a design value of flow rate G:

$$f = \xi \qquad \text{– if } G_- \leq G \leq G_+$$
$$f = \xi + \min\left[\left(G - G_\pm\right)^2\right]/\varepsilon \qquad \text{– otherwise}$$

where ε is the penalty coefficient, usually prescribed in a way that the objective function sharply rises to infinity with the increasing distance from the limits of the assumed range of variation. As the pressure drop during optimisation is kept constant and the mass flow rate is constrained in a very narrow range of variation, any change of power of the optimised stage is due to the reduced flow losses only.

Flow computations are made with the help of computer code FlowER [8] and ANSYS CFD [9] where turbulent flow of compressible viscous gas is described by 3D RANS equations. Turbulence effects are modeled using the k-ω SST (shear stress transport) model [10]. Discretisation of governing equations is made by the finite volume method. A second-order upwind based scheme is selected for numerical solution. The calculations converge to a steady state. A mixing plane approach is used to treat the relative motion of the stator and rotor, based on circumferential averaging of flow parameters in the axial gaps between the blade rows. The assumed boundary conditions are typical for turbomachinery calculations, including no slip and zero heat flux at the walls, as well as spatial periodicity at the borders of the flow channel. The pressure drop across the stage (stage group) is imposed. Therefore, for a given flow geometry, the mass flow rate is resultant.

The calculations are carried out in one blade-to-blade passage of the stator and rotor refined near the endwalls, blade walls (y^+ = 1-2), leading and trailing edges. Due to large costs of RANS computations, coarse grids are used in the course of optimisation. After optimisation, the original and optimised geometries are recalculated on refined grids.

The following parameters of blade shape can be considered during the optimisation for each blade row:

– blade height, blade number and stagger angle,
– a number of blade profile parameters, or alternatively a number of camber line and blade thickness parameters (at different blade sections),
– a number of endwall contour parameters,
– a number of 3D blade stacking line parameters.

In this paper, parametrisation of the blade profile, camber line or endwall contour is made using a set of circle arcs or Bezier functions. The idea of blade profile description by means of circle arcs is well-known. Several groups of stator and rotor profiles, such as N1-N3, PLK and R1-R3 profiles are built based on the set of 3 to 7 circle arcs on the pressure and suction surface of the profile, [11]. Each arc is determined by its circle centre coordinates and radius. Subsequent arcs remain tangent to each other. The pressure and suction surface are linked by two more circle arcs which form the leading and trailing edge of the profile.

Also, approximation of blade profiles by means of Bezier functions for optimisation is popular among turbomachinery society [2, 3]. In this work, a special form of Bezier functions, that is a rational Bezier function is used [12]. The shape of a Bezier curve is affected by its control points and their weights. For a 3-rd order Bezier function ($n = 3$) each curve is defined by 4 control points – 2 end points and 2 internal points, 4-th order Bezier curve has 5 control points. A weight is prescribed to each control point. Subsequent Bezier curves are assumed tangent to each other to make the pressure and suction surface of the profile smooth. During optimisation, the shape of the profile is varied by varying Bezier curves and their parameters.

3. Hybrid stochastic-deterministic optimisation methods

Typical deterministic methods of optimisation such as the direct search method of Hooke-Jeeves [13] and the simplex method of Nelder-Mead [14] are effective for objective functions having a single extremum. However, they may not be effective in case of multimodal functions having a number of extrema as they tend to reduce the range of search and hold on to a local extremum. Stochastic methods such as genetic algorithms [15], simulated annealing [16], swarm intelligence [17] or bat algorithm [18] are very reliable in finding global extrema of multimodal functions. Unfortunately, the stochastic methods have a low rate of convergence in the vicinity of the extremum, which largely increases computational costs of optimisation. A solution may be the application of hybrid stochastic-deterministic schemes [19, 20].

Simulated annealing Hooke-Jeeves method:

This hybrid scheme is a modification of the Hooke-Jeeves method, which includes elements of classical simulated annealing. Similar to the original Hooke-Jeeves scheme, two stages of calculations can be distinguished: trial and working stage.

In the trial stage, the vicinity of a base point is searched along all directions of the ortogonal coordinate system. If the trial stage is successful, in the working step the old base point is moved to a new base point. If not, the Metropolis test is performed. A random number r is generated from the interval [0,1] and compared against $p = \exp(-\delta f/T)$, where δf is a local increase of the objective function, T is the control parameter called temperature. If $r<p$ then the best point obtained in the trial step is accepted as a new base point. The random factor thus introduced enables the algorithm to go beyond the local extremum.

The entry data for this hybrid algorithm are:

n – number of parameters (dimension of the objective function),

$\boldsymbol{x}^0$ – starting point,

τ – initial step length,
$\alpha = 0.8$ – step reduction coefficient,
T – temperature,
ϵ – termination criterion.
Bat algorithm with a simplex:
This hybrid method starts with a bat algorithm so as to approach the vicinity of the global extremum. The stochastic algorithm evolves from echolocation behaviour of bats, while finding their prey. The search is made by varying pulse rate and loudness of emission and intensified by random walk. Typical entry data for the bat algorithm are:
n – number of parameters (dimension of the objective function),
$\boldsymbol{x}_{i,min}$, $\boldsymbol{x}_{i,max}$ – lower and upper boundaries of the search region,
Ngen – generation number,
Npop – population,
A – loudness,
r – pulse rate,
Q – scale factor,
RanGen – model of random number generator,
M – maximum number of iterations.

After a prescribed number of iterations, the best point is selected and an initial simplex for the Nelder-Mead method is built around it. Typical entry data for the Nelder-Mead method are:
n – number of dimensions,
$\boldsymbol{x}^{(0)}$, L_{simp}– initial point and width of the regular simplex,
α, γ, β, σ - reflection, expansion, contraction and reduction coefficient,
ε - termination criterion.

Typical test cases for testing optimisation schemes are the chained Rosenbrock (banana-valley) function or multimodal trigonometric function [21]. The effectiveness of some hybrid stochastic-deterministic methods of optimisation was illustrated in [3].

4. Optimisation of blade profiles in a low-load HP turbine stage

The HP turbine stage selected for optimisation comes from a 200 MW steam turbine and operates at a pressure drop from 42 to 38 bar (pressure ratio $p_{ex}/p_{in} = 0.9$) and at a mass flow rate 57 kg/s. This low reaction stage consists of a stator and rotor with cylindrical (straight) blades and PLK / R2 profiles. The stator and rotor profiles are described by a set of circle arcs. 12 free parameters of profile arcs plus two stagger angles of the stator and rotor blade were selected for optimisation. The objective function was the enthalpy loss including the exit energy. The penalty was imposed on the changes of mass flow rate larger than $\pm 0.5\%$, as compared to the original operating flow rate.

The optimisation was conducted using the simulated annealing Hooke-Jeeves method. The shape of the original and modified (optimised) profiles is illustrated in Fig. 1. Changes of shape of the stator blade are relatively small, slightly increasing the profile camber, thus increasing the flow turning within the cascade. Changes in

the rotor are more visible. The rotor profile becomes thicker. The stagger angles of the stator and rotor blades did not change.

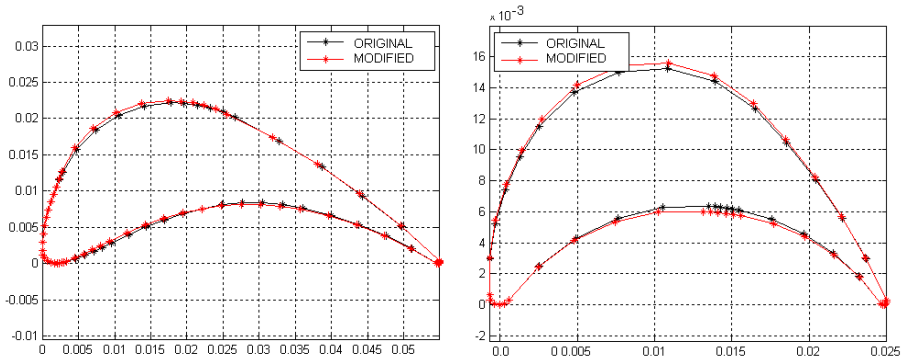

Figure 1 Original and modified geometry of the stator (left) and rotor blades (right)

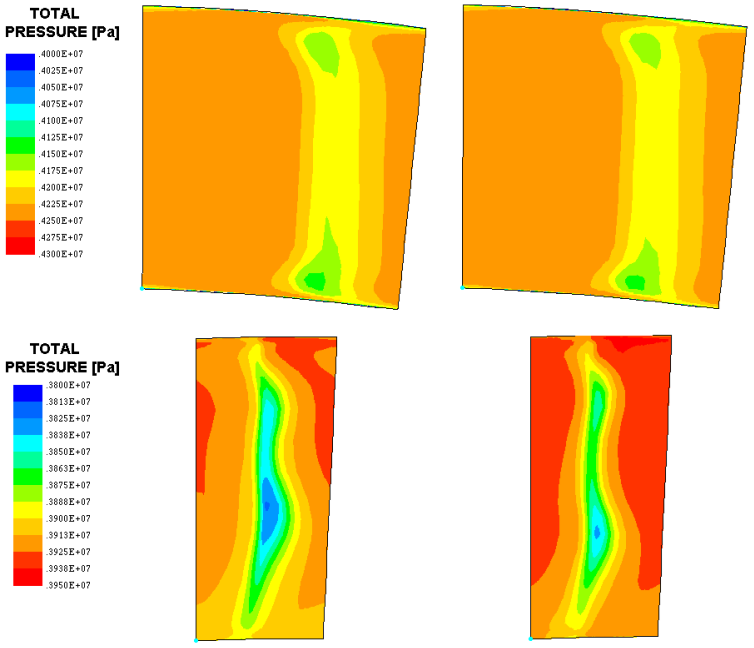

Figure 2 Total pressure contours downstream of the stator (top) and rotor (bottom): original geometry (left), modified geometry (right)

As a result of optimisation the objective function was decreased by 0.8% point. The obtained efficiency gains can be explained using field contours and loss distributions in the stator and rotor [22]. Total pressure contours shown in Fig. 2 indicate a better expansion in the cascades and a reduction in the intensity of endwall flows, especially in the optimised rotor cascade, whose blades become more aft-loaded. The calculated stage losses are decreased both without the exit energy and with the exit energy (by 0.8% point from 10.4% down to 9.6%). Optimisation of the profile shape leads to the improvements both in 2D and 3D flow through the turbine cascades.

5. 3D optimisation of a radial-axial turbine rotor

The optimised radial-axial turbine rotor comes from a single stage small power (50 kWe) ORC turbine operating on silica oil MM. ORC technology is especially suitable for cogeneration based on biomass and recovery heat [23-25]. The turbine was designed using a 0D approach in Matlab 2016a environment [26]. Thermodynamic properties of MM were found from NIST REFPROP library [27]. The flow efficiency of the turbine was estimated at 87.9% (not including tip leakage losses). Design parameters of this turbine are given in Tab. 1. The turbine consists of 16 nozzles and 15 rotor blades. A meridional section of the flow channel is displayed in Fig. 3 whereas a 3D turbine model is shown in Fig. 4.

Table 1 Design parameters of the radial-axial turbine operating on silica oil MM

Parameter	Value
Rotational velocity [rpm]	28000
Inlet pressure [kPa]	1109
Inlet temperature [K]	448
Outlet pressure [kPa]	20
Mass flow rate [kg/s]	0.68
Power [kW]	50

Parametrisation of 3D geometry of this radial-axial turbine consists in determination of the blade angle along the profile camber line and determination of endwall contours at the hub and tip by means of 4-th order Bezier curves with 5 control points, Fig. 5. The blade angle distribution was given from the leading to the trailing edge at three spanwise locations. The endwall contours were assumed axisymmetrical. 35 parameters of blade angle distribution and endwall contours were varied during optimisation. The total-to-static efficiency (η = 1-ξ) was assumed as an objective function. Turbine design parameters such as mass flow rate and power were constrained in a very narrow range of variation.

The comparison of the optimized and original geometry is illustrated in Fig. 6. The optimized geometry has a bowed blade, which is especially clear at the trading edge. The rotor blade also has an increased height at the trailing edge. The total-to-static efficiency was increased from 87.9% to 89.6%, that is by 1.7 % point. Turbine design parameters such as mass flow rate and power were found not to change.

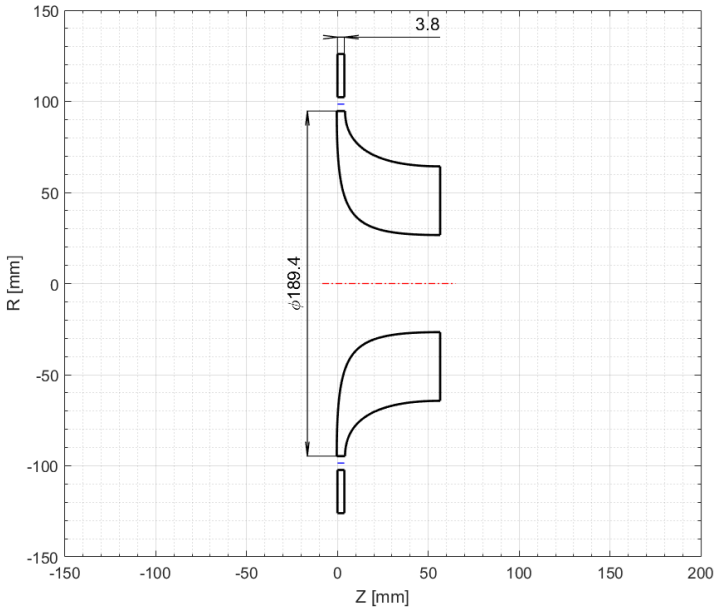

Figure 3 Meridional section of the radial-axial turbine flow domain

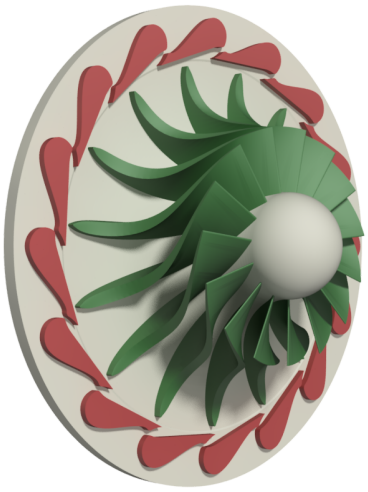

Figure 4 Radial-axial turbine

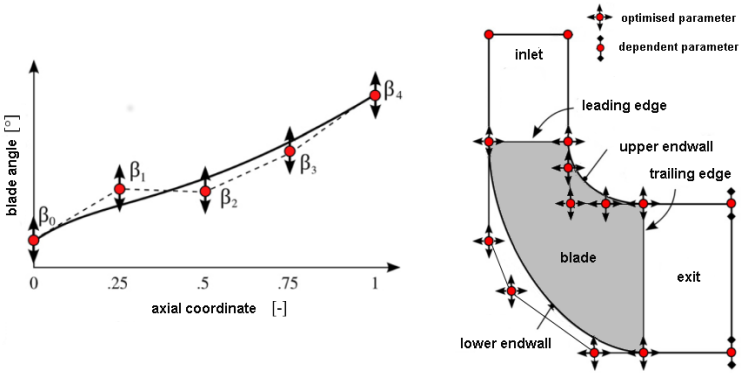

Figure 5 Bezier curves for sample blade angle distribution of along the camber line (left), lower and upper endwall in meridional view (right) [28]

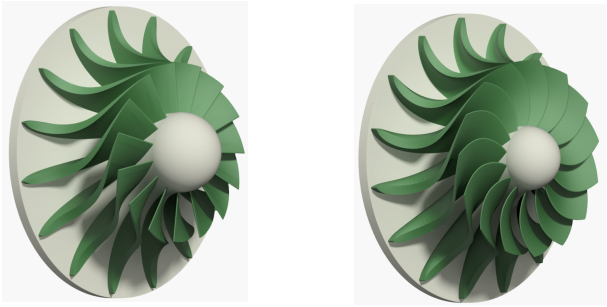

Figure 6 3D model of the original (left) and optimised (right) rotor

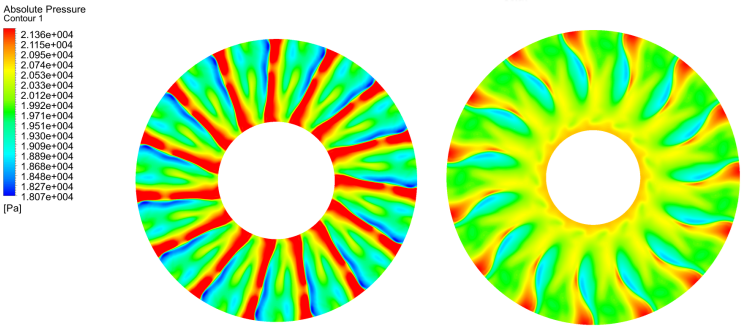

Figure 7 Comparison of total pressure contours behind the original (left) and optimized (right) rotor

The comparison of total pressure contours downstream of the trailing edge of the original and optimized rotor blade presented in Fig. 7 shows a significant redistribution of total pressure losses in the flow channel resulting in decreased loss at the suction side of the optimised rotor blade and in the central part of the channel due to a considerable reduction of blade and secondary flow vortices. On the other hand, losses at the pressure surface of the optimized rotor are increased. The comparison of streamlines illustrated in Fig. 8 shows an improvement in flow pattern at the suction side of the optimized rotor, which confirms the decreased loss regions at the suction surface observed in the earlier figure.

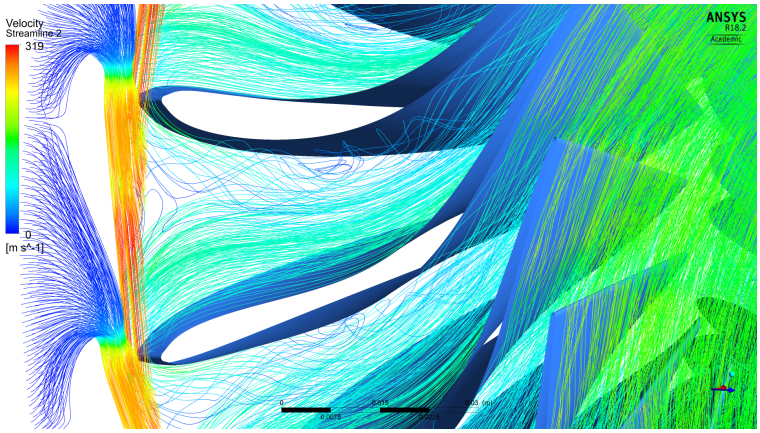

Figure 8 Comparison of streamlines in the original (left) and optimised (right) rotor

6. Conclusions

The paper describes the idea of direct constrained optimisation of flow systems in the turbomachinery environment. The final shape of the blading is obtained from minimising the objective function, which is the total enthalpy loss of the turbine stage found from 3D RANS computations. There are constraints imposed on the mass flow rate, exit swirl angle and reactions as well as on changes of stresses in the metal. The optimisation is carried out using hybrid stochastic-deterministic methods such as a combination of a direct search method of Hooke-Jeeves and simulated annealing or a combination of a bat algorithm and simplex method of Nelder-Mead. Among free shape parameters were blade number and stagger angle, blade profile parameters and endwall contour parameters.

Two practical examples of turbine flow optimisation were presented in the paper. First, low load profiles PLK-R2 for an HP stage of a 200 MW steam turbine were optimised. Almost 1% efficiency increase was obtained from optimisation of HP blade profiles, especially by making the rotor blade more aft-loaded and reducing the intensity of endwall flows. An ORC radial-axial cogeneration turbine of 50 kWe

was also optimised. Almost 2% efficiency rise was obtained for the optimised turbine due to flow improvement at the suction side of the blade and reduction of blade and secondary flow vortices.

7. Acknowledgements

Part of this work was supported by The National Science Centre,
Grant No. 2015/17/N/ST8/01782.

References

[1] **Chmielniak T., Łukowicz H., Kochaniewicz A.**: Kierunki wzrostu sprawności współczesnych bloków energetycznych, *Rynek Energii*, 6, 79, 14–20, **2008**.

[2] **Pierret S., Van Den Braembussche R.**: Turbo-machinery blade design using a Navier-Stokes solver and artificial neural network, *ASME*, Paper 98-GT-4, **1998**.

[3] **Lampart P., Hirt Ł.**: Complex multidisciplinary optimisation of turbine blading systems, *Arch. Mech.*, 64, 2, 153–175, **2012**.

[4] **Denton J.D.**: Loss mechanisms in turbomachines, *ASME J. Turbomachinery*, 115, 621–656, **1993**.

[5] **Lampart P., Yershov S., Rusanov A.**: Increasing flow efficiency of high-pressure and low-pressure steam turbine stages from numerical optimisation of 3D blading, *Engineering Optimisation,* 37, 2, 145–166, **2005.**

[6] **Arabnia, M., Ghaly, W.**: On the use of blades stagger and stacking in turbine stage optimization, *ASME*, Paper GT2010-23399, **2010**.

[7] **Asgarshamsi A., Hajilouy-Benisi A., Assempour A., Pourfarzaneh A.**: Multi-point optimization of lean and sweep angles for stator and rotor blades of an axial turbine, *ASME*, Paper GT2014-27016, **2014**.

[8] **Yershov S., Rusanov A.**: The application package FlowER for the calculation of 3D viscous flows through multi-stage turbomachinery, Certificate of state registration of copyright, *Ukrainian state agency of copyright and related rights*, February 19, **1996**.

[9] ANSYS CFD Software, *https://www.simutechgroup.com/ansys-software*.

[10] **Menter F.R.**: Two-equation eddy-viscosity turbulence models for engineering applications, *AIAA J.*, 32, 8, 1598–1605, **1994**.

[11] **Dejcz M.,E., Filippov G.A., Lazarev L.Ja.**: Atlas of axial turbine cascade profiles, *Machine Construction*, Moscow (in Russian), **1965**.

[12] Bezier curve, *http://www.wikipedia.org/Bezier curve*.

[13] **Hooke R., Jeeves T.A.**: Direct search solution of numerical and statistical problems, *J. Assoc. Computing Machinery*, 8, 2, 212–229, **1961**.

[14] **Nelder J.A., Mead R.**: A simplex method for function minimisation, *Computer J.*, 7, 1, 308–313, **1965**.

[15] **Goldberg D.E.**: *Genetic Algorithms in Search, Optimization and Machine Learning*, Addison-Wesley Longman Publishing Co. Inc., Boston, MA, USA, **1989**.

[16] **Kirkpatrick S., Gelatt C., Vecchi M.**: Optimisation by simulated annealing, *Science, New Series*, 220(4598), 671–680, **1983**.

[17] **Clerc M.**: Particle Swarm Optimization, *John Wiley & Sons*, **2006**.

[18] **Yang X. S.**: A New Metaheuristic Bat-Inspired Algorithm, in: Nature Inspired Cooperative Strategies for Optimization, *Studies in Computational Intelligence*, 284, 65–74, **2010**.

[19] **Chelouah R., Siarry P.**: A hybrid method combining continuous tabu search and Nelder-Mead Simplex algorithms for the global optimisation of multiminima functions, *Europ. J. Operational Research*, 161, 636–654, **2005**.

[20] **Mahmuddin M., Yousof Y.**: A Hybrid Simplex Search and Bio-Inspired Algorithm for Faster Convergence, *Proc. Int. Conf. on Machine Learning and Computing*, Perth, Australia, 203–207, **2009**.

[21] **Pardalos P. M., Romelin H. E.**: Handbook of global optimization, Vol. 2, Nonconvex optimization and its application, *Kluwer Academic Publishers, Boston/Doordrecht/London*, **2002**.

[22] **Lampart P.**: Investigation of endwall flows and losses in axial turbines, Part II. The effect of geometrical and flow parameters, *J. Theoret. Appl. Mech.*, 47, 4, 829-853, **2009**.

[23] **Wajs J., Mikielewicz D., Bajor M., Kneba Z.**: Experimental investigation of domestic micro-CHP based on the gas boiler fitted with ORC module, *Arch. Thermodynamics*, 37, 3, 79–93, **2016**.

[24] **Borsukiewicz-Gozdur A.**: Influence of the ORC power plant heat recuperation solutions on effectiveness of the supplied waste heat utilization, *Arch. Thermodynamics*, 31, 4, 11–124, **2010**.

[25] **Kiciński J., Żywica G.**: Steam Microturbines in Distributed Cogeneration, *Springer International Publishing*, **2015**.

[26] **Klonowicz P., Surwiło J., Witanowski Ł., Suchocki T.K., Kozanecki Z., Lampart P.**: Design and numerical study of turbines operating with MDM as working fluid, *Open Engineering*, 5, 1, 485–499, **2015**.

[27] **Lemmon E., Huber M., McLinden M.**: REFPROP, National Institute of Standards and Technology, **2010**.

[28] **Mueller L., Alsalihi Z., Verstraete T.**: Multidisciplinary Optimization of a Turbocharger Radial Turbine, *ASME J. Turbomachinery*, 135, 2, 021022, **2012**.